

REVIEW OF HIGH-BRIGHTNESS PROTON & ION ACCELERATION USING PULSED LASERS*

J.Fuchs[#], P. Audebert, P. Antici, E. Brambrink, E. d'Humières, J.-C. Gauthier, L. Romagnani,
Laboratoire pour l'Utilisation des Lasers Intenses, UMR 7605 CNRS-CEA-École Polytechnique-
Université Paris VI, 91128 Palaiseau, France

T.E. Cowan, A. Kemp, N. Renard-LeGalloudec, H. Ruhl, Y. Sentoku, Physics Department, MS-220,
University of Nevada, Reno, Nevada 89557, USA

M. Borghesi, C.A. Cecchetti, School of Mathematics and Physics, The Queen's University, Belfast,
United Kingdom

O. Willi, T. Toncian, A. Pipahl, Institut für Laser und Plasmaphysik, Heinrich-Heine-Universität,
Düsseldorf, Germany

P. Mora, Centre de Physique Théorique, UMR 7644 CNRS-Ecole Polytechnique, 91128 Palaiseau,
France

E. Lefebvre, DPTA, CEA-DIF, Bruyères-le-Châtel, France

I. Barton, J. Kaae, R. Stephens, General Atomics, San Diego, CA 92121, USA

M. Roth, A. Blazevic, M. Geissel, Gesellschaft für Schwerionenforschung, 64291 Darmstadt,
Germany

M. Hegelich, J. Cobble, J.C. Fernández, University of California, Los Alamos National Laboratory,
Los Alamos NM 87545, USA

M. Kaluza, S. Karsch, J. Schreiber, Max-Planck-Institut für Quantenoptik, 85748 Garching,
Germany

V. Malka, M. Manclossi, Laboratoire d'Optique Appliquée – ENSTA, UMR 7639, CNRS, Ecole
Polytechnique, 91761 Palaiseau, France

S. Meyroneinc, Centre de Protonthérapie d'Orsay, BP 65, 91402 Orsay, France

H. Pépin, INRS-ÉMT, 1650 bd. L. Boulet, J3X1S2 Varennes, Québec, Canada

Abstract

Laser-accelerated ion sources have exceptional properties, i.e. high brightness and high spectral cut-off, high directionality and laminarity, short burst duration. A review of these properties, that open new opportunities for ion beam generation and control, and could stimulate development of compact ion accelerators for many applications, is presented.

INTRODUCTION

Laser-acceleration of intense, collimated beams of multi-MeV protons [1] is a fast growing area of high-field science that is very promising for a number of applications. The generation of such beams has been only recently achieved [2,3,4] since it requires extremely high laser intensities that are now available thanks to the fast progress of short-pulse lasers [5]. The first experiments all reported a well-defined proton beam in the forward direction (with respect to the laser pulse) with a roughly exponential spectrum and mean energy in the MeV range and a high-energy cut off in the 10-55 MeV range. The

beam was generally emitted with a low divergence angle (max. $\sim 20^\circ$), with the most energetic protons having the lowest divergence angle, along the normal to the rear target surface.

Due to its pulsed nature (the duration at the source is of the order of \sim ps), its extremely high beam quality [6,7], the high number of protons (10^{11} - 10^{13} ions in a single bunch) that can be produced and the possibility to tailor the spectrum [8,9,10] and the beam divergence [10,11], the laser-proton source could prove useful for applications. Energetic proton beams are already applied for high-resolution charged-particle radiography [12]. Another potential application could be to use these beams to ignite [13,14] pre-compressed capsules in the "Fast Ignitor" [15] scenario of inertial confinement fusion or, in a broader perspective, to produce warm-dense matter [11]. Other perspectives include high-brightness injectors for accelerators [7], and sources for proton therapy [16,17,18] or radioisotope production [19]. Since the first observations, particular attention has been devoted to the exceptional accelerator-like spatial quality of the beams, and current research focuses on their optimisation (energy, divergence, spectrum).

*Work supported by by grant E1127 from Région Ile-de-France, EU program HPRI CT 1999-0052, LANL Laboratory Directed Research & Development, corporate support of General Atomics and UNR grant DE-FC08-01NV14050.

[#]julien.fuchs@polytechnique.fr

ACCELERATION MECHANISMS

As illustrated in Fig.1, the high-current, collimated multi-MeV beams of protons are generated by irradiating thin solid foils with ultra-intense ($> 10^{18}$ W.cm⁻²) short-pulse lasers (30 fs -10 ps) produced by the chirped pulse amplification (CPA) technique [20]. We will not discuss here of the mechanisms leading to ion acceleration in lower density plasmas [21] since they tend to produce lower-energy ions with a low beam quality.

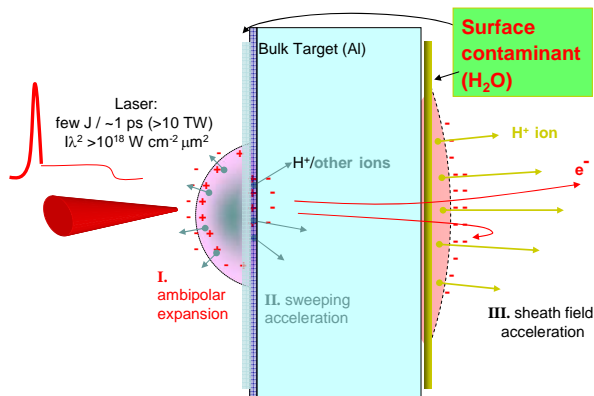


Figure 1: Schematic of the various mechanisms leading to laser-acceleration of high-energy ions by a short, high-intensity laser pulse irradiating a thin target.

Up to the presently accessible highest laser intensities, the dominant mechanism that leads to acceleration of high energy protons from solids in the forward direction occurs at the non-irradiated (rear) surface [22,23,24,25]. There, relativistic electrons laser-accelerated from the front side into the target form a dense electron plasma sheath. At the laser-intensities considered here, since the electrons are generated at the target front side with mean energies in the MeV range, their mean-free path is much larger than the typical target thickness (a few tens of microns). Therefore, the electrons can cross the target material and exit into vacuum. Most of the electrons are however retained at the target surface due to the potential that has built within the target. The charge-separation field that results from the formation of the sheath on the rear surface of the target is initially of the order of a few TV/m over a Debye length ($\lambda_D \sim 1\mu\text{m}$ in the solid target for a hot electron temperature ~ 1 MeV). This field ionizes the surface atoms almost instantaneously and rapidly accelerates ions in the direction normal to the initially unperturbed surface [26]. The accelerated beam is composed mostly of protons originating primarily from contaminant layers of water vapor and hydrocarbons on the target surface [27,23]. Together with the electrons that were part of the initial sheath, the ions expand in vacuum. As the laser is switched off, the electrons cool down by adiabatic energy transfer to the ions [28], leading to a decrease of the driving electric field [29]. The electrons eventually drift at the same velocity as the ions and the ion energy saturates, leading to a sharp high-energy cut-off [28], as observed in all experiments [1].

In case heating of the target was performed prior to the experiments in order to eliminate the hydrogen contaminants as much as possible, the acceleration of heavier ions is favoured [8].

BEAM CHARACTERISTICS

Energy and particle number

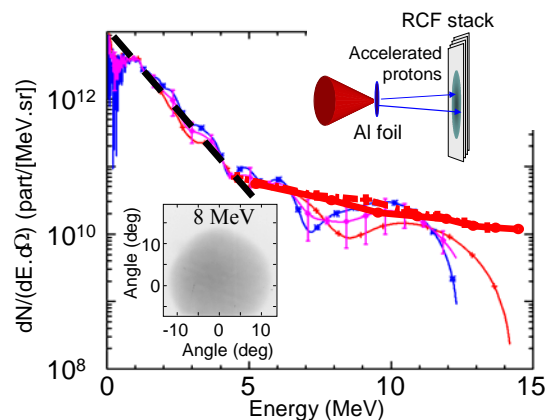


Figure 2: Typical spectrum of protons laser-accelerated from a 20 μm thick Al foil irradiated by a $3 \cdot 10^{19}$ W.cm⁻², 350 fs laser pulse, as measured by Faraday cups using time-of-flight techniques (thin lines) or stacks of radiochromic films (RCFs, thick lines). Top insert: Experimental set-up. The accelerated protons are collected in a stack of RCFs positioned 3 cm after the target. Bottom insert: transverse beam profile as recorded in the stack for protons with a mean energy of 8 MeV.

The high energy proton beams accelerated this way have fundamentally different properties from lower energy protons observed in earlier work at lower laser intensity with laser pulses in the nanosecond regime [27], which were accelerated from the coronal plasma and emitted into a large solid angle. They exhibited strong trajectory crossing and a broad energy spectrum with typical ion temperatures of ~ 100 keV/nucleon. These unspectacular characteristics prevented major applications. On the contrary, as illustrated in Fig.2, beams accelerated by ultra-intense laser pulses exhibit a high number of ions per bunch (spread however over a large spectrum), a limited divergence (the beam is emitted in a well-defined cone), an extreme laminarity, and a high cut-off energy. The emission is along the normal to the un-irradiated rear surface of the target.

A review of the maximum energy and proton number obtained in various experiments is shown in Fig.3. Fig.3.a shows the evolution of the recorded maximum proton energy as a function of the pulse duration. The data have been grouped so that similar conditions (e.g. similar laser intensities) in experiments carried out in different laboratories could be compared. Fig.3.a shows clearly that the maximum proton energy increases with the laser pulse duration, the increase following roughly parallel lines for varying laser irradiances. The lines overlaid on the plot for various

laser intensities represent the scaling given by a simple model which has been confronted to a systematic series of experiments [30]. Fig.3.b shows that not only the maximum proton energy but also the efficiency of the acceleration process increases with the laser pulse duration and the laser irradiance. Here we have not calculated a global energy conversion from laser to protons since the data reported in the various experiments differ in terms of spectral energy range so that a consistent number cannot be compared for the various experiments. The point of comparison is the number of protons with 10 MeV of energy accelerated in the forward direction. When this number increases, the total delivered dose, and hence the conversion efficiency, increases [30].

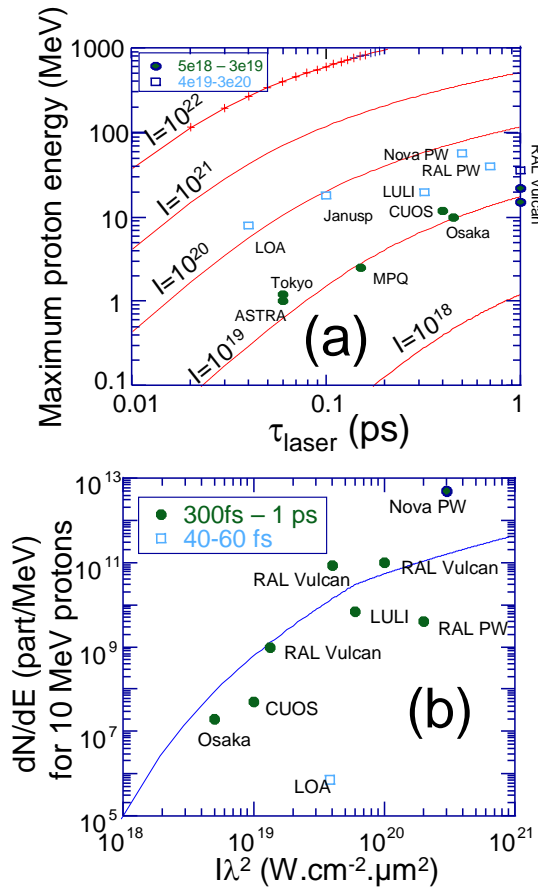


Figure 3: Review of (a) cut-off maximum proton beam energy and (b) number of protons in a 1 MeV bin around 10 MeV as reported from published data. In (a) dots and squares are experimental data for the two intensity ranges shown in the legend box, the intensities are in units of W.cm⁻². Lines represent calculations following the model detailed in Ref. [30] for various laser intensities, as indicated in units of W.cm⁻², assuming 20 μm thick targets and a 10 μm FWHM laser spot size. In (b) dots and squares are experimental data for the two laser pulse duration ranges shown in the legend box. The line is still given by the same model assuming 20 μm thick targets, a 10 μm FWHM laser spot size and a 0.5 ps duration laser pulse.

Angular characteristics and emittance

Since the ions are accelerated by the electron sheath on the target rear surface, their spatial and angular characteristics are determined by the electron sheath spatial distribution. Therefore the protons' spatial and angular characteristics depend on the target material, the target surface roughness [31], the target shape, and the laser focal distribution on target.

In the case of controlled, ideal conditions for the laser and the target, i.e. a conductor target, a mirror-like smooth target surface, and a smooth laser focal distribution, it is observed that the proton beam exhibits a smooth angular distribution [32] with a sharp boundary (see Fig.2). If one imagines that the electron sheath follows a generic bell-shaped spatial distribution, both the existence of a sharp angular boundary in the proton angular distribution and the decrease of the beam divergence with its energy are easily understood. Indeed, the higher energy protons are accelerated from the tip of the sheath with a very small divergence angle. The acceleration of lower energy protons corresponds to exploring the wings of the sheath. As the ions are accelerated normal to the electron density iso-contours, ions of lower energy will have larger divergence than the ones accelerated from the sheath tip since they correspond to the sides of the sheath. This is clearly observed experimentally [3].

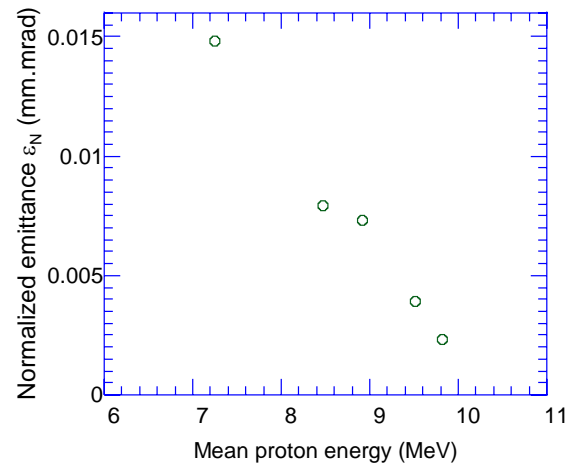


Figure 4: Normalized rms emittance, as a function of the mean proton energy, inferred from the radiochromic films recording the proton beam pattern (shown in Fig. 2.a-c of Ref. [7]) accelerated from an 18 μm thick Al flat target irradiated by a 10^{19} W/cm², 800 fs laser pulse.

Deviations from the ideal conditions mentioned above will perturb the proton angular distribution. Using an insulator target, a roughened target surface, or a modulated laser focal spot will produce an unsmooth proton beam.

The unique and most interesting characteristics of the laser-accelerated proton beam lie in their high degree of laminarity, or equivalently their extremely low source size. This is the key factor that enables potential applications, and that renders these sources

potentially interesting as high-brightness injectors for accelerators. This is most precisely measured by producing fiducials of the beam flow. Such fiducials are produced by purposefully micro-machining shallow grooves on the target surface. Doing this produces a periodic modulation of the beam angular envelope [7,33]. As protons are first accelerated normal to the surface, the grooves on the surface induce a modulation of the take-off angle. Due to the global sheath expansion, an overall near-linear divergence is added to this initially imprinted angular modulation of the beam. Projected on a film stack far away, this results in a modulation of the proton dose. Using such modulations of the beam intensity, it is possible to image the proton-emitting surface, to reconstruct the transverse phase-space of the beam flow, and to determine the transverse emittance, as illustrated in Fig.4. Fig.4 gives the root-mean-square (rms) value of the “normalized emittance” ε_N , at a specific beam energy. The transverse emittance ε_N corresponds to the area of the bounding phase-space (here x - p_x for beam propagation along z) ellipse that is $\pi\varepsilon_N$. The emittance is expressed as $\varepsilon_N = (\mathbf{p}/mc) [\langle x^2 \rangle \langle x'^2 \rangle - \langle xx' \rangle^2]^{1/2}$ where m is the ion mass, c is the velocity of light, x is the particle position within the beam envelope and $x' = p_x/p_z$ is the particles' divergence. Fig.4 shows that for protons of up to 10 MeV, the transverse emittance is as low as 0.0025 mm.mrad, i.e. 100-fold better than typical RF accelerators and at a substantially higher ion current (kA range). It is important to note that this value is actually an upper limit that is limited by the experimental technique of producing the fiducials in the beam flow and that the real emittance could be even lower.

It has also been shown [34] that the removal of the co-moving electrons after 1 cm of the quasi-neutral (protons and electrons) beam expansion did not increase significantly the measured proton transverse emittance. This last observation is important since, in order to take advantage of the exceptionally small proton beam emittance in future applications, e.g. to capture them into a post-accelerator, removal of the co-moving electrons without significantly perturbing the protons is crucial.

The exceptionally low measured emittance stems from the extremely strong, transient acceleration that takes place from a cold, initially unperturbed surface and from the fact that during much of the acceleration the proton space charge is neutralized by the co-moving hot electrons.

Regarding the longitudinal emittance, the energy spread of the laser-accelerated proton beam is large, from 0 to tens of MeV, however due to the extremely short duration of the accelerating field (<10 ps), the longitudinal phase-space energy-time product is probably less than 10^{-4} eV.s. A good longitudinal velocity “chirp” of the beam is important since it could allow producing monochromatic beams by coupling the beam to the field gradient of a post-accelerator.

Beam handling

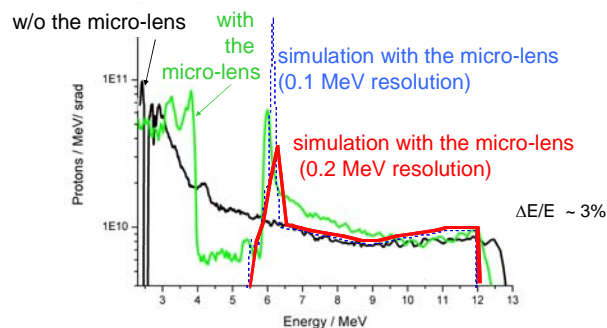


Figure 5: Proton spectra showing the energy selection capability of a plasma-based, laser-triggered proton micro-lens [10].

An important requirement for many applications is to be able (i) to refocus the beam on a target or to collimate it to transport it over large distances, and (ii) to select a sufficiently small energy spread $\Delta E/E \ll 1$ out of the energy spectrum of the beam.

Focusing at short distances (a few 100s of microns) has been achieved by curving the target surface in order to focus down the protons to a tight spot [11].

For energy selection, there are already several options. First, it has been proposed to use combinations of conventional deflecting magnets with selecting apertures to pick only a fraction of the broad initial energy distribution that is subsequently refocused for dose delivering [35]. Research at JAEA-KPSI (Japan) is exploring phase-space rotation. Alternatively, it is also possible to achieve energy selection by using double layer targets with a heavy ion layer followed by a thin proton layer. In this case, simulations [36] have shown that a small energy spread can be achieved if the proton layer is thin enough so that it is depleted before the accelerating field decreases. This scheme, recently demonstrated using micro-structured targets [8,9], however requires complex target engineering.

A different and interesting option to solve the two issues mentioned above simultaneously is to use an ultrafast laser-triggered micro-lens [10]. This device provides tuneable, simultaneous focusing and energy selection of MeV proton beams. The principle of operation is rather simple: the micro-lens is a hollow cylinder that is irradiated by an auxiliary laser pulse. This pulse injects relativistic electrons through the cylinder's wall. These electrons spread evenly on the cylinder's inner walls and initiate hot plasma expansion. The radially symmetric transient electric fields associated with the expansion can act to focus protons transiting along the axis of the cylinder. This device that can selectively focus a part of the proton beam allows for tunable energy selection of the energy spectrum by positioning appropriate apertures downstream in the beam, as demonstrated in Fig.5.

Such relativistic laser-plasma device appear very suitable to achieve the required angular and spectral

control of laser-accelerated ion beams since it can withstand large ion beam currents, can be switched over ps time scales, and can support large deflecting fields on micro-scales.

PROSPECTS

The main challenge that face laser-accelerated ion beams is ion energy increase. Simply scaling the known mechanisms to higher laser energy shows (see Fig.3) that several hundred MeV protons could be achievable with foreseeable future high-power lasers [30]. Such lasers, in order to be compact and have a (necessary) high repetition rate, will rely on innovations like diode-pumping systems [37,38] which also represent a major step in increasing the overall efficiency of laser light production. According to scaling models [30,39], there seems to be an optimum laser pulse duration in the range ~200 fs- 1 ps to accelerate the highest energy ions; this duration represent a matching of the energy transfer time between hot electrons and ions. Regarding the issue of the available proton flux per laser shot, still using the same scalings [30] the number of protons around 200 MeV which could be produced by a laser pulse of 0.5 ps duration, $8 \cdot 10^{20}$ W.cm⁻² intensity, and 3 μ m FWHM focal spot irradiating a 10 μ m thick target would be $\sim 10^9$ particles in a $\Delta E/E=10^{-2}$ bin for a single laser shot.

Energy increase may also be provided by exploiting the relativistically transparency regime where simulations [40] show that proton acceleration should be even more efficient. In this scheme, the laser pulse interacts with the whole volume of a very thin, dense target and this can accelerate the whole electron population efficiently. This however requires ultra thin targets and therefore ultra-high contrast pulses. Preliminary experiments show the potential of such interaction regime [30].

Simulations performed at higher laser intensities than presently achievable suggest that other mechanisms than the currently explored ones could accelerate ions at high energy. For example, ions could be trapped and accelerated in the bulk of the target by an ion shock induced by the ponderomotive pressure of the laser on the target front surface [40]. Simulations indicate that for laser pulses with intensities roughly $I > 10^{21}$ W.cm⁻², and for optimal target thicknesses, shock-accelerated protons could be more energetic than the ones accelerated from the rear surface. At even higher laser intensities (up to $\sim 10^{23}$ W.cm⁻²), there could be a transition to another extreme ion acceleration regime [41]. In this mechanism, the radiation pressure of the electromagnetic wave is directly converted into ion energy via the space-charge force related to the displacement of the electrons in a thin foil. Achieved proton energies would be in the GeV region.

REFERENCES

[1] M. Borghesi et al., Fusion Science and Technology 49 (2006) 412.

- [2] E. Clark et al., Phys. Rev. Lett. 84 (2000) 670.
 [3] R. Snavely et al., Phys. Rev. Lett. 85 (2000) 2945.
 [4] A. Maksimchuk et al., Phys. Rev. Lett. 84 (2000) 4108.
 [5] G. Mourou et al., Rev. Modern Phys. 78 (2006) 309.
 [6] M. Borghesi et al., Phys. Rev. Lett. 92 (2004) 055003.
 [7] T. Cowan et al., Phys. Rev. Lett. 92 (2004) 204801.
 [8] B. M. Hegelich et al., Nature 439 (2006) 441.
 [9] H. Schwoerer et al., Nature 439 (2006) 445.
 [10] T. Toncian et al., Science 312 (21 April 2006) 410.
 [11] P. Patel et al., Phys. Rev. Lett. 91 (2003) 125004.
 [12] A. Mackinnon et al., Rev. Sci. Inst. 75 (2004) 3531.
 [13] M. Roth et al., Phys. Rev. Lett. 86 (2001) 436.
 [14] M. Temporal et al., Phys. Plasmas 9 (2002) 3098.
 [15] M. Tabak et al., Phys. Plasmas 1 (1994) 1626.
 [16] A. Boyer et al., Physics Today (Sept. 02 issue) 34.
 [17] S.V. Bulanov et al., Physics Letters A 299 (2002) 240.
 [18] E. Fourkal et al., Med. Phys. 29 (2002) 2788.
 [19] M. Santala et al., Appl. Phys. Lett. 78 (2001) 19.
 [20] D. Strickland, and G. Mourou, Opt. Comm. 56 (1985) 219.
 [21] K. Krushelnick et al., Phys. Rev. Lett. 83 (1999) 737; S. Fritzler et al., Phys. Rev. Lett. 89 (2002) 165004; K. Matsukado et al., Phys. Rev. Lett. 91 (2003) 215001; X. Wang et al., Phys. Plasmas 12 (2005) 11301; L. Willingale et al., Central Laser Facility Rutherford Appleton Laboratory annual report (2005) 8, ISBN 0902376365.
 [22] J. Fuchs et al., Phys. Rev. Lett. 94 (2005) 045004.
 [23] M. Allen et al., Phys. Rev. Lett. 93 (2004) 265004.
 [24] T. Lin et al., Proc. of the Advanced Accelerator Concepts Conference, AIP conf. Proc. 737 (2004) 595.
 [25] M. Kaluza et al., Phys. Rev. Lett. 93 (2004) 045003.
 [26] S. Hatchett et al., Phys. Plasmas 7 (2000) 2076.
 [27] S.J. Gitomer et al., Phys. Fluids 29 (1986) 2679.
 [28] P. Mora, Phys. Rev. E 72 (2005) 056401.
 [29] L. Romagnani et al., Phys. Rev. Lett. 95 (2005) 195001.
 [30] J. Fuchs et al., Nature Physics 2 (2006) 48.
 [31] M. Roth et al., Phys Rev ST-AB 5 (2002) 061002.
 [32] J. Fuchs et al., Phys. Rev. Lett. 91 (2003), 255002.
 [33] H. Ruhl et al., Phys. Plasmas 11 (2004) L17.
 [34] T. Cowan et al., Nucl. Inst. And Methods in Physics Research A 544 (2005) 277.
 [35] E. Fourkal et al., Med. Phys. 30 (2003) 1660.
 [36] T. Esirkepov et al., Phys. Rev. Lett. 89 (2002) 175003.
 [37] J. Hein et al., Appl. Phys. B 79 (2004) 419.
 [38] J.C. Chanteloup et al., Proc. SPIE 5707 (2005) 105.
 [39] J. Schreiber et al., submitted (2006).
 [40] E. d'Humières et al., Phys Plasmas 12 (2005) 062704.
 [41] T. Esirkepov et al., Phys. Rev. Lett. 92 (2004) 175003.